A novel pan class-I glucose transporter inhibitor DRB18 exhibits synergistic effects *in vitro* and *in vivo* with paclitaxel against human non-small cell lung cancer

Pratik Shriwas[1-3], Lindsey Bachmann[1,3,4], Ryan Ward[1,3,4], Subhodip Adhicary[1,5], Corinne M. Nielsen[1,2,5,6], Yunsheng Li[3], Haiyun Zhang[1-3], Jingwen Song[1-3], Dennis Roberts[8], Stephen Bergmeier[2,8], Xiaozhuo Chen[1-3,7-9]

1 Department of Biological Sciences, Ohio University, Athens, Ohio, USA
2 Program of Molecular and Cellular Biology, Ohio University, Athens, Ohio, USA
3 Edison Biotechnology Institute, Ohio University, Athens, Ohio, USA
4 Honors Tutorial College, Ohio University, Athens, Ohio, USA
5 Translational Biomedical Sciences Program, Ohio University, Athens, Ohio, USA
6 Neuroscience Program, Ohio University, Athens, Ohio, USA
7 Department of Biomedical Sciences, Ohio University, Athens, Ohio, USA
8 Department of Chemistry and Biochemistry, Ohio University, Athens, Ohio, USA
9 Heritage College of Osteopathic Medicine, Ohio University, Athens, Ohio, USA

Key Words: Anticancer therapeutics, GLUT, Combinatorial therapy, Glucose transport and metabolism, synergism, Paclitaxel

Correspondence to

Xiaozhuo Chen
109 Edison Biotechnology Institute
Ohio University
172 Water Tower Drive, the Ridges
Athens, Ohio 45701
USA
Email: chenx@ohio.edu
Cell Phone: 01-740-274-9200

Running title: DRB18 and Paclitaxel exhibit synergism in NSCLC *in vitro* and *in vivo*

Conflict of interest disclosure statement: The authors declare no potential conflicts of interest.

Abstract

Cancer cells depend on glucose for biomass synthesis, cell proliferation, and drug resistance. Glucose transporter (GLUT) transcripts as well as proteins are upregulated in human lungs and other cancers and are negatively correlated with patient survival. Thus, inhibiting GLUT function has been an attractive anticancer strategy. We previously characterized WZB117 and DRB18, first- and second-generation pan-class I GLUT inhibitors, respectively. DRB18 strongly inhibits glucose transport mediated by GLUT1-4 in non-small lung cancer (NSCLC) A549 cells *in vitro* and *in vivo*. Here, we report DRB18 as a more stable and potent anticancer compound, compared to WZB117. DRB18 reduced glucose uptake in NSCLC A549, pancreatic Panc1, and cervical Hela cancer cells with varied but strong anticancer potencies in the presence or absence of extracellular nutrients such as ATP and glucose. Combined with different clinical and pre-clinical anticancer compounds such as V9302, CB839, Sutent, Brigatinib, DRB18 significantly increased death of A549 and Panc1 cells. Noteworthy, DRB18 exhibited strong anticancer synergy with paclitaxel, an approved chemo drug for NSCLC, drastically reducing cancer cell proliferation *in vitro* and growth of A549 tumors grafted on the flank of nude mice without increased side effects, compared to single drug treatments. Mechanistically, dual treatment of DRB18 with paclitaxel elevated the expression of Caspases 3 and 9, suggesting GLUT-inhibiting and apoptosis-inducing anticancer mechanisms of DRB18 with paclitaxel. Collectively, our results demonstrate anticancer efficacy of DRB18 either working alone or in combination with paclitaxel, providing a potentially more efficacious therapeutic strategy for treating advanced NSCLC and other cancers.

Introduction

Lung cancer is the second most common cancer among men and women in the United States (1), with non-small cell lung cancer (NSCLC) contributing to more than 80% of all lung cancer cases (2). Currently, major therapeutic strategies for NSCLC include chemo or targeted therapy and immune therapy, with chemotherapy remaining the gold standard in NSCLC treatment (3, 4). Despite these different therapies, the five-year survival rate of NSCLC remains under 30% (2). Major issues in lung cancer therapy include resistance developed to therapy, and side-effects at higher dosages of drugs (5, 6). It has been established that combinatorial drug therapies are more effective in treating different types of cancers and induce less drug resistance than single drug therapies (7, 8). It has been reported that drug resistance in cancer, including NSCLC, are closely associated with glucose transport and glucose metabolism (9, 10).

Glucose uptake and anerobic glycolysis are drastically upregulated in different cancer types for the synthesis of biomass, energy production, and cell proliferation. This phenomenon is known as the Warburg effect (11-13). Glucose uptake is mediated by a group of plasma membrane-spanning protein channels called glucose transporters (GLUTs) (14-16). GLUT1 is the main GLUT in most human cells and most cancer cells, internalizing glucose to satisfy the energetic requirements of the cell (17, 18). It is well known that GLUTs, particularly class I GLUTs (GLUT1-4), are either inducible or co-expressed with GLUT1 in different types of cancer (33, 34). Further studies show that these GLUTs possess unique, but also partially redundant, functions with each other and frequently compensate in case of single GLUT inhibition, making successful single-GLUT or specifically GLUT1 targeting more challenging.

Consequently, targeting glucose transport and metabolism, via inhibiting GLUTs, becomes an attractive anticancer strategy (19-21). Recently, many different GLUT inhibitors have been developed and tested (22-25) in pre-clinical models. WZB117, a first-generation lead

inhibitor synthesized in our labs (26-28), has shown anticancer activity across several cancers via reducing drug resistance and epithelial mesenchymal transition (EMT) of cancer cells (29-31) as well as exhibiting additive anticancer effects, *in vitro* and *in vivo*, in combination with FDA-approved drugs (32).

We recently showed that knocking out the *GLUT1* gene in NSCLC A549 cells did not reduce tumor growth in Nu/J mice (38), suggesting that other class-I GLUTs might have compensated for the lost GLUT1 activity. In contrast, simultaneous inhibition of multiple GLUTs, by second-generation lead GLUT inhibitor DRB18 (38), appears to be a far more effective strategy to block glucose transport and glucose metabolism, ultimately leading to increased cancer cell death. Demonstrated by a molecular docking study, DRB18 binds human GLUT1-4 in an outward open conformation (38), exhibiting glucose uptake inhibitory IC_{50}s varying from 0.9 µM to 9 µM among human GLUT1-4 (38). DRB18 reduced growth in A549 xenograft tumors at 10 mg/kg body weight, when administered intraperitoneally daily for five weeks (38).

Observing the targeting of pan Class I GLUTs and the improved anticancer efficacy of DRB18, we hypothesized that DRB18 could potentially be used in combination with approved anticancer drugs to achieve synergistic anticancer efficacy. During combinatorial therapy, we lowered the dosages of DRB18 and paired anticancer agents and achieved greater tumor inhibitory activities, with lower side effects of each compound. These results show profound implications for using DRB18, alone or in combination with approved anticancer drugs, to generate more effective anticancer therapies with significantly reduced side effects.

Materials and Methods

Compound inhibitors and other chemicals

Compounds WZB117 and DRB18 were synthesized as previously reported (26,35). Compound solutions were freshly prepared by dissolving the compounds in dimethyl sulfoxide (DMSO) before each experiment. Adenosine 5-triphosphate disodium salt hydrate (A2383), D-(+)-Glucose (G7021), L-glutamine solution 200 mM (59202-C), Paclitaxel (T7402), Sunitinib malate (PZ0012), and Resazurin sodium salt (R7017) were purchased from Sigma Aldrich**.** Brigatinib (19778) and Trametinib (16292) were purchased from Cayman chemicals. V9302 (HY-112683) and CB839 (HY-12248) were purchased from MedChemExpress. Dulbecco's Modified eagle Medium (DMEM) high glucose (ATCC-30-2002), Eagle's Minimum Essential Medium (EMEM-ATCC 30-2003), RPMI (ATCC-30-2001), Fetal bovine serum (ATCC-30-2020), and Penicillin-Streptomycin Solution (ATCC-30-2300) were purchased from American Type Culture Collection (ATCC). DMEM (no glucose, no glutamine) was purchased from Thermo Fisher Scientific (A1443001). Deoxy-D-glucose, 2-[1,2-3H(N)], 250 µCi (37 MBq) was purchased from Perkin Elmer (NET549250UC). Stock concentrations of compounds were prepared by dissolving compounds in DMSO or Ethanol. The working solutions of the compounds were prepared by diluting stock solutions in appropriate cell culture media.

Cell lines and experimental controls

All cell lines were purchased from ATCC and were grown in growth media supplemented with 10% FBS and 1% penicillin/streptomycin (Pen/strep). Dulbecco's Modified eagle Medium (DMEM) was growth media for A549, H1299, and Panc1 cells, EMEM for HOP92 and Hela cells while INS-1 cells were cultured in RPMI-1640 (39). All the cells were grown in a cell culture incubator with 5% CO_2 at 37^0C. Mock (DMSO/Ethanol) treated samples served as negative controls.

Glucose uptake assay in cancer cells and in specific GLUT-expressing cell lines

Glucose uptake inhibitory activity of DRB18 was analyzed using radioactive 2-deoxy-d-[^{3}H] glucose as previously described (26,36). For initial seeding density of 40000 cells per well were used for all cell lines but 100,000 cells for INS-1 cells.

Cell proliferation assays

Cell proliferation assays were performed using resazurin as a fluorescent dye as previously described (38). For cell viability assays for extracellular nutrients, an appropriate amount of glucose, glutamine or ATP was added to the DMEM (no glucose/no glutamine) supplemented with 10% FBS and 1% pen/strep to prepare assay media. The cells were then treated with different concentrations of compounds or nutrients for 24, 48, or 72 hours. After treatment, the media was removed from cells and cell viability was measured using resazurin dye.

Intracellular ATP assay

25,000 A549, Panc1 or Hela cancer cells were seeded in each well of 96 well black plate. Intracellular ATP levels in the cancer cells were measured as described previously (38).

WZB117/DRB18 stability assay

WZB117 and DRB18 were pre-incubated at 37°C in 1 ml cell culture media at 30 µM concentration for different times (0-72 hours). A549 cells were seeded at 5,000 cells per well in a 96-well plate. Cells were then treated for 24 hours with the WZB117 or DRB18 pre-incubated solution. For the control, 0.1% DMSO was used to treat the cells for 24 hours. The cell viability was measured by a resazurin assay as described above.

DRB18 synergism assay

5,000 A549/Panc1 cells were seeded in each well of 96-well plates. Cells were treated with appropriate concentrations of compounds for 24 or 48 hours. Cell viability was measured using resazurin dye as described above. Synergy score analysis was performed using SynergyFinder ver3.0 (https://synergyfinder.fimm.fi). An HSA model was used to determine synergism based on synergy scores, which were interpreted using the following baselines: score < -10: antagonistic, score between -10 and 10: additive; score >10: synergistic**.**

Western blot analysis

Western blot analysis was performed as previously described (26,38). Antibodies used were rabbit anti-Caspase-3 (1:1000, CST-9662), and rabbit anti-Caspase 9 (1:1000, CST-9502). Rabbit anti-Cofilin (1:5000, CST-5175) and rabbit anti-Vinculin (1:3000, CST-4650) were used as loading controls.

Bioinformatics analysis

mRNA/correlation/overall survival analysis of human GLUTs was performed using data collected from cbioportal (https://www.cbioportal.org/).

Immunohistochemistry study of human LUAD array

Fixed, paraffin-embedded human lung tissue samples (LC486, LC1531, HuCAT232, HuFPT178) (Tissue Array) included Stage I-IV lung adenocarcinoma and tumor/cancer adjacent controls. To prepare tissue sections for antibody staining, samples were deparaffinized in xylenes, rehydrated in ethanol series, and subject to antigen retrieval using 10 mM sodium citrate + 0.05% Tween-20 at sub-boiling temperature (microwave oven), incubated in 3% hydrogen peroxide to quench endogenous peroxidase, and blocked in 5% donkey serum in 0.1% Tween-20 buffer. Rabbit anti-GLUT1/SLC2A1 (1:200, Proteintech 21829-1-AP) or Rabbit anti-GLUT3/SLC2A3 (1:50, AbClonal A8150) primary antibodies were applied in blocking

reagent overnight at 4°C. HRP-conjugated donkey anti-rabbit (1:100, Cell Signaling 7074P2) secondary antibody was applied in blocking reagent for 2 hours at room temperature. For chromogen precipitation, 1% DAB chromogen (Electron Microscopy Sciences) + 0.3% hydrogen peroxide was applied for ~5 min before reaction was stopped and tissue sections were mounted with Permount (Fisher). Patient characteristics are given in the Supplementary Table 2-5.

Animal study

The animal experiments were performed in accordance with guidelines for animal care by the NIH and IACUC protocol approved by Ohio University.

4 weeks old male *Nu/J* mice were purchased from Jackson Laboratories and were put on Irradiated Teklad Global 19% rodent (protein) diet from Harlan Laboratories. The protocols for subcutaneous injection of tumors (tumor generation), intraperitoneal administration of compounds/vehicles, weekly tumor measurements, body weight/food intake measurements and animal euthanasia were performed as previously described (26, 38). Briefly, mice were allowed to acclimatize for one week after arrival. They were injected with $5x10^6$ A549 cells subcutaneously on the flank. The tumors became palpable after 3 days at ~100 mm^3 volume. Mice were divided into 4 groups: Group I: control group (n = 8) treated with PBS/DMSO (1:1, v/v); Group II: 8 mg/kg (body weight) DRB18 treatment group (n = 7); Group III: 8 mg/kg (body weight) paclitaxel treatment group (n = 8); Group IV 8 mg/kg DRB18 + 8mg/kg paclitaxel treatment group (n = 8). Tumor volume, body weight and food intake were measured weekly for all the groups. The mice were euthanized after 5 weeks of treatment and final tumor volume and body weight were measured. Tumor volume was calculated by the formula; $V= LW^2/2$ where L=Length, W= Width.

Data processing and statistical analysis

For all the cell and molecular studies, each experimental condition was performed in triplicates or quadruplets and the experiment was repeated at least once. For animal studies, the data is represented as mean ± standard error of the means (SEM). Other data is reported as mean ± standard deviation (STD) and analyzed using Student's two-tailed *t*-test. $P \leq 0.05$ was considered significant.

Results

3-1. GLUT1 and GLUT3 are major contributing GLUTs in lung adenocarcinoma

GLUT1 and *GLUT3* mRNA expression levels were found to be higher in tumors of human patients, compared to benign samples (Figure S1A and S1B). Thus, we investigated the expression of GLUT1 and GLUT3 in human lung adenocarcinoma (LUAD) cancer tissue microarray of LUAD patients of different stages (Supplementary table T2-T5). We found that GLUT1 expression was increased in Stages I & II tumors compared to normal lung tissue, and GLUT1 was upregulated in tumor samples of higher stage patients (Figure 1A-B). Similarly, we found that GLUT3 was increased in tissue adjacent to tumor tissues of Stage I & II, but it was not further increased in higher stage samples (Figure 1C). In addition, we found that the expressions of GLUT1 and GLUT3 were higher in grade 3 tumors compared to grade 2 (CPTAC, APOLLO 2022 LUAD cohort n=87) (Figure S1C and S1D). Further investigation of the TCGA-firehose legacy clinical dataset revealed that *GLUT1* mRNA was increased in higher stage (T3-T4) patients compared to lower stages (T1-T2) as well as in patients with nodal metastasis (N1/N2/N3) compared to those without (N0) (Figure 1D-E). However, *GLUT3* mRNA was not increased significantly in higher stage patients as well as patients with nodal metastasis (T3-T4) (Figure S1E-F). Next, we found that LUAD patients from TCGA cohort which had higher *GLUT1* and *GLUT3* mRNA had poorer survival compared to those with lower expression (Figure

1F). Individually, only higher *GLUT1* mRNA and not *GLUT3* had poorer survival compared to those with lower expression (Figure S2A-B) (http://gepia.cancer.pku.cn/). Further, we found that expressions of GLUT1 and GLUT3 were positively correlated in TCGA-LUAD (mRNA) and CPTAC 2020 (protein) (Figure 1G-H). However, *GLUT4* was found to be negatively correlated with both *GLUT1* and *GLUT3* mRNA levels in the TCGA-LUAD cohort (Figure S2C-D). In the CCLE database (Broad Institute, 2019) GLUT1 and GLUT3 were found to be positively correlated at mRNA and proteins levels in overall cancer types as well as lung cancer (Figure S2E-H). We further found that *GLUT3* mRNA had the highest mutations (8%) among *GLUT1-4* in TCGA-LUAD cohort using OncoPrint tool in cbioportal (Figure S3A). Copy number alterations in *GLUT3* mRNA expression levels in TCGA-LUAD cohort were increased significantly in patients with gain/amplifications and diploid compared to patients with deletions (Figure S3B). Protein-protein interaction study using genemania (https://genemania.org/) identified 20 major interacting partners of GLUT1 and GLUT3 (Figure S3C). Similarly, string database analysis revealed p53 as a major interacting partner of GLUT1 and CREB1 for GLUT3 (Figure S3D). Gene Ontology (GO) analysis using shinyGOv0.741 (http://bioinformatics.sdstate.edu/go74/) using the top interacting partners for GLUT1 and GLUT3 revealed NADH regeneration, canonical glycolysis, and glucose catabolism to pyruvate as major GO: biological processes; glucokinase, hexokinase, and fructokinase were major GO: molecular functions (Figure S3E-F). Overall, these analyses indicated that GLUT1 and GLUT3 proteins are overexpressed in LUAD and have direct effect on survivability.

3-2. DRB18 is a more stable and potent anticancer compound than WZB117

Previously, we reported two glucose transporter inhibitor compounds (Figure 2A) WZB117 (26-28) and DRB18 (35-38), which can target multiple cancers and have demonstrated anticancer potency in pre-clinical studies. To investigate the stability of these compounds, WZB117 and

DRB18 were pre-incubated in serum-containing cell culture media for 0-72 hours and then A549 cells were treated with the compound's solutions for 24 hours. While DRB18 retained its antiproliferative potency for the full duration of 72 hours, WZB117 showed decreased potency at approximately 12 hours, and completely lost its anticancer activity after 48 hours (Figure 2B-C). Furthermore, DRB18 had a much higher proliferation-inhibitory activity at 10 μM against 9 major cancer types compared to WZB117 (Figure 2D). Since DRB18 was a more potent multi-GLUT-targeting compound, we focused on DRB18 in this study. DRB18 reduced cell viability in A549 cells in a time-dependent manner (Figure 2E). Furthermore, we found that DRB18 reduced glucose uptake in many different cell lines in a dose-dependent manner (Figure 2F). Further, we tested the acceptability of DRB18 as therapeutic agent by using swissadme portal (http://www.swissadme.ch/index.php). We found that DRB18 had a bioavailability score of 0.55 and drug likeliness based on Lipinski score and high GI absorption. These suggest DRB18 is a possible drug candidate (Supplementary Table 1).

3-3. DRB18 potency in cancer cells is affected by the availability of extracellular nutrients

To investigate if the potency of DRB18 can be altered by the presence of extracellular nutrients, which directly or indirectly affect central carbon metabolism, we performed different *in vitro* assays in A549, Panc1, and Hela cells, with varying concentrations of glucose, glutamine, and ATP. We firstly found that intracellular ATP levels were dependent on extracellular glucose (25 mM or 5mM) and extracellular ATP (eATP). Furthermore, DRB18 reduced intracellular ATP (iATP) in dose-dependent manner (0, 10 and 20 μM) and its activity also depended on extracellular glucose and eATP (Figure 3A-C). Next, when we treated A549 cells with varying concentrations of glucose (0-40 mM) in the presence and absence of 10 μM DRB18, and we found that the potency of DRB18 inhibition increased in the presence of higher glucose concentration and further quantification of inhibitory differences showed that DRB18 cytotoxicity

towards A549 cells depended directly on extracellular glucose (Figure 3D-E). Next, we repeated the same experiment in different concentrations of extracellular glutamine (0-4 mM) and found that extracellular glutamine did not have any significant effect on DRB18 potency but 0 mM glutamine drastically reduced A549 cell viability (Figure 4F). Similar experiments were performed using extracellular glucose and glutamine in Panc1 cells. We found that extracellular glucose, but not glutamine, had an impact on DRB18 cytotoxicity towards Panc1 cells (Figure 2G-I). These analyses suggest that DRB18 mediated inhibition of cell proliferation via inhibition of glucose transport, is dependent on eATP and extracellular glucose, and relies to a lesser extent on extracellular glutamine.

3-4. DRB18 exhibits synergistic effects with anticancer compounds *in vitro*

To investigate the clinical applicability of DRB18, we tested synergistic effects of the compound with other anticancer drugs, which were either in clinical use or used in pre-clinical models. We found that glucose and glutamine can synergistically reduce cell viability in A549 and Panc1 cells (Figure S4A and S4B). Based on these results, the glutamine transporter inhibitor V9302 and glutaminase I inhibitor CB839 were used in both the cell lines. We first determined the IC_{50} of V9302 and CB839 in both cell lines (Figure S4C-F). We found that the combination of 10 µM DRB18 and 10 µM V9302 showed more inhibitory activity towards A549 and Panc1 cells in comparison to no treatment or single treatment of both compounds (Figure 4A and 4D). Similarly, dual treatment of DRB18 and CB839 showed significantly more cytotoxicity in A549 and Panc1 cells (Figure 4B and 4E). Sunitinib is an FDA approved receptor tyrosine kinase inhibitor in different cancer types. We found that 10 µM DRB18 exhibited additive effect with sunitinib at both 5 and 10 µM in both A549 and Panc1 cells (Figure 4C and 4F). Brigatnib is an FDA approved drug for metastatic NSCLC. We determined the IC_{50} of brigatinib in A549 cells (Figure S4G). We further found that 5 µM DRB18 showed no additive effect with 0.5 µM

brigatinib, but the combined treatment of 5 µM DRB18 and 0.75 µM brigatinib was able to reduce cell viability in A549 cells significantly more than control or either compound working alone (Figure 4G). Trametinib is an FDA approved drug for treatment of melanoma and NSCLC and is a MEK inhibitor. We determined the IC_{50} of trametinib in A549 cells (Figure S4H) and found that 5 µM DRB18 and 15 µM of trametinib exhibited additive effects in A549 cells, although no such effect was observed between DRB18 and 10 µM trametinib (Figure 4H).

3-5. DRB18 exhibits synergistic effects with Paclitaxel *in vitro*

Paclitaxel is an FDA approved drug for metastatic NSCLC and is known to target tubulin polymerization in lung cancer cells (40-42). We tested the potential synergism of DRB18 with paclitaxel in A549 and Panc1 cells. We found that 10 µM DRB18 and 10 µM paclitaxel showed synergism, by inhibiting cell growth in A549 cells after 48 hours of treatment with varying dosages of paclitaxel (Figure 5A-C). We computed synergism by using synergyfinder (synergyfinder.org) and used an HS model to determine the synergism score of 17.56 ($P \leq 0.001$). We tested administration of 10 µM DRB18 and 10 µM Paclitaxel in Panc1 cells and found that dual treatment reduced cell growth significantly after 48 hours, compared to either single compound or control (Figure 5D). Since DRB18 reduces glucose transport and leads to glucose deprivation in cancer cells, we wanted to determine whether low glucose conditions could exhibit synergism with paclitaxel in A549 and Panc1 cells. We found that dual treatment of 1 µM paclitaxel and low glucose (2 mM) conditions inhibited cell growth in A549 cells more significantly than either condition alone (Figure 5E). This effect was not observed at 0.3 µM paclitaxel concentration. However, in Panc1 cells, both 0.3 and 1 µM paclitaxel in low glucose (2 mM) conditions were able to reduce cell growth significantly more than in either condition alone (Figure 5F).

3-6. DRB18 exhibits synergistic effects with paclitaxel *in vivo*

We next wanted to test if the combination of DRB18 and paclitaxel was synergistic *in vivo*. Nude mice were implanted with subcutaneous injections of A549 cells and then were treated with either vehicle, 8 mg/kg DRB18, 8 mg/kg paclitaxel, or combined DRB18+paclitaxel for 5 weeks. We found that dual treatment of DRB18 and paclitaxel significantly reduced the tumor volume by approximately 79%, 73%, and 50% in comparison to vehicle, DRB18 alone, and paclitaxel alone, respectively (Figures 6A-B). Comparing the final tumor weights, they were reduced by approximately 87%, 85%, and 71% in comparison to vehicles, DRB18 alone, and paclitaxel alone, respectively (Figure 6C). We also observed that there was no significant reduction in the average body weight of the mice in the four groups as well as no differences in food consumption over the 5-week span from the start of the treatment (Figures S5A-B). We then investigated the possible mechanism of action of this synergy by western blot analysis from the harvested xenografts. It was found that apoptosis-inducing protein caspase 9 and caspase 3 were significantly increased in dual treatment, compared to single compound or vehicle (Figure 6D-E).

4. Discussion

4-1. Most cancers upregulate class I GLUTs, and DRB18 is a pan-class I GLUT inhibitor

GLUTs play critical roles in cellular homeostasis by ensuring adequate supply of glucose as main source of energy and carbon to mammalian cells (14-16). GLUTs, particularly pan-class I GLUTs, have been found to be upregulated in many cancer types and are responsible for a wide variety of functions such as proliferation, drug resistance and metastasis (33, 34, 43). Previously, we reported that a pan-class I GLUT inhibitor, DRB18, reduced GLUT-mediated glucose transport and energy metabolism and cell viability *in vitro* and *in vivo* against human

lung cancer cells (38). In this study, we first performed analyses to further confirm expression status of GLUTs and their potential roles in cancer patients.

Immunohistochemistry of the human tumor microarray from LUAD samples showed that expression of GLUT1 and GLUT3 was increased in lower stage (I-II) and higher stage (II-IV) lung tumors compared with the normal lung tissues (Figure 1A). However, only GLUT1 was increased between lower to higher stage LUAD patient specimens (Figure 1B-C). Similarly, GLUT1 and GLUT3 protein expression was increased in another TCGA-LUAD cohort (Figure S1C-D). In addition, *GLUT1* mRNA was also increased in higher stage as well as patients with nodal metastasis while *GLUT3* mRNA was not (Figure 1D-E; S1E-F). These conclusions are further supported by the TCGA-firehose legacy cohort analysis where patients with higher *GLUT1* and *GLUT3* mRNA had significantly poorer survival to those with lower mRNAs (Figure 1F). Correlation analysis showed that *GLUT1* and *GLUT3* transcript expressions were positively correlated in LUAD patients (Figure 1G) as well as GLUT1 and GLUT3 proteins were also positively correlated in CPTAC 2020 dataset (Figure 1H). Further, this positive correlation exists in CCLE dataset of *in vitro* cell lines from lung cancer as well as combined different cancer types (Figure S2E-H). These data collectively suggest that although GLUT1 and GLUT3 are overexpressed in lung cancer cells and are upregulated in LUAD patients, GLUT1, one of the major targets of DRB18 (38), is more important of the two GLUTs in LUAD. Further identification of key interacting partners of GLUT1 and GLUT3 and gene ontology analysis of these proteins revealed that glucose transport and glycolysis are key pathways via which GLUTs alter the cellular metabolism (Figure S3C-F) and thus targeting GLUTs becomes an attractive anticancer strategy.

Although inhibiting glucose transport and glucose-mediated metabolism, in theory, should be effective in inhibiting tumor growth, most cancer cells express more than one GLUT (44,45), and

they are known to play different roles in tumor growth and metastasis. Recently, we reported that DRB18 is a pan-class I GLUT inhibitor that acts on GLUT1-4 with variable inhibitory potency (38). In addition, tumors generated from A549 cells lacking *GLUT1* (A549 *GLUT1* knockout cells) grew just as fast as regular A549-generated tumors (38). These results suggest that some other class I GLUTs (GLUT2-4) might have compensated for the lost function of GLUT1 in A549-GLUT1KO tumors. In contrast, DRB18 inhibited A549 tumor growth due to its pan class I GLUT-targeting activity (38).

4-2. Cancers use alternative pathways to bypass drug treatment, and combinational therapy with DRB18 can overcome this problem

Cancers have their built-in flexibility in bypassing enzyme / pathway inhibitions and generating resistance to a treatment with mono anticancer therapy. A combinatorial therapy with two anticancer drugs, including a GLUT inhibitor such as DRB18, will be much more advantageous over single drug therapies when the cancer growth relies on glucose transport and on another cell-growth signaling pathways that are unrelated to glucose transport / glucose metabolism.

Personalized monotherapy using chemo or targeted drugs are still prevalent in the clinic. However, the major concern associated with single drug therapy is toxicity due to higher drug dosages and induced drug resistance, resulting in tumor relapses after initial remission. Cancer cells are dependent on multiple mechanisms for survival. It becomes necessary, therefore, to target multiple mechanisms simultaneously for better therapeutic outcomes. Thus, identifying and using combo therapy in a synergistic combination is imperative to reduce the burden of high drug dosages as well as undesired side-effects of each drug in a drug pair.

4-3. Anticancer synergism between DRB18 and paclitaxel

The main criterium for synergism between two drugs is that the anticancer of two drugs working together can achieve a superior efficacy to the total sum of the individual anticancer efficacies of the drug pair working alone. Synergy is relatively rare to find between two anticancer agents and is difficult to predict *in vitro* and even more so *in vivo*.

In this study, we report the additive or synergistic effects of DRB18 along with other FDA approved or clinically tested anticancer drugs. Investigation of DRB18 properties revealed (**http://www.swissadme.ch**, 04 January 2024) that DRB18 has a positive Lepinski score, good gastrointestinal absorption, and a high bioavailability score of 0.55, further justifying its potential as a drug candidate (Supplementary Table 1). One of the major objectives of this study was to investigate the synergistic mechanisms of DRB18 with other clinical or preclinical anticancer agents. Among anticancer drugs and compounds tested, we found paclitaxel to be the most suitable candidate for forming a synergistic pair with DRB18. Paclitaxel is the gold standard chemotherapy drug for advanced NSCLC and for patients who are sensitive to immunotherapy. Paclitaxel has several properties to make it suitable as a drug candidate, but sometimes monotherapy fails due to drug induced toxicity such as neurotoxicity (46-48). Therefore, it becomes necessary to identify compounds synergistic with paclitaxel, so that the drug pair can reduce paclitaxel dosage while significantly improving anticancer efficacy.

During tumor treatment, no adverse effects were observed, including no differences in food intake and body weight (Figure S5A-B) in the DRB18+paclitaxel group, compared with the DRB18 group or paclitaxel group. This might be due to dosage and/or administration intervals of the drugs we used. In our previous tumor studies, 10 mg/kg was used for DRB18 (38), whereas the generally used dosage for paclitaxel is 10 mg/kg. In the pilot and full-scale studies of this investigation, 8 mg/kg for both DRB18 and paclitaxel was used and found to be effective in reducing tumor growth, without adverse effects on body weight and food intake. Additional fine-

tuning adjustments in dosages and drug administration frequency may further improve the treatment results.

Taken together, our data demonstrated that human lung cancers overexpress GLUT1 and GLUT3, while our pan-class I GLUT inhibitor DRB18 inhibits GLUT1-4 (36). Thus, DRB18 is a wide spectrum inhibitor for class I GLUTs and GLUT-upregulating NSCLC and other cancers. While working alone, DRB18 reduced tumor size of NSCLC A549 cells. The combinatorial therapy of DRB18 and paclitaxel further reduced the size of tumors significantly, showing anticancer synergy. Moreover, these adjustments led to no significant changes in food intake and body weight, compared with mock-treated controls. Thus, DRB18, as a pan-class I GLUT inhibitor, can function alone or in combination with other approved anticancer drugs to treat different cancers, as paclitaxel has been approved for treating eight different cancers, to achieve greater anticancer efficacy. Additionally, more approved anticancer drugs will likely be identified to exhibit synergy with DRB18, further widening the applications of DRB18 or pan class I GLUT inhibitors in cancer therapies. These may significantly increase the use and values of the pan class I GLUT inhibitors in new cancer therapies. Noteworthy, GLUT4 has recently been found implicated in aging and neuronal diseases such as Alzheimer's and Parkinson's (49), further expanding DRB18's utility in treating human diseases beyond cancers.

Figure legends

Figure 1. GLUT1 and GLUT3 were prognostic markers for lung adenocarcinoma patients. 1A. IHC analysis of human patient tissue microarray shows comparison between normal lung tissue versus lower stages (Stage I and II) and higher stages (III-IV) for GLUT1 and GLUT3 proteins**. 1B.** Quantification of GLUT1/tissue area for normal, lower stages (I and II) and higher stages (III and IV)**. 1C.** Quantification of GLUT3/tissue area for normal, lower stages (I and II)

and higher stages (III and IV)**. 1D.** *GLUT1* mRNA was increased in patients from lower stages (Stage T1-T2; n=198) to higher stages (Stage T3-T4; n=32) in TCGA-LUAD cohort. **1E.** *GLUT1* mRNA was increased in patients with no nodal metastasis (N0; n=333) compared to those with nodal metastasis (N1/N2/N3; n=172) in TCGA-LUAD cohort. **1F**. Overall survival of patients in TCGA-LUAD cohort decreased with increasing *GLUT1* and *GLUT3* mRNA expression. **1G**. *GLUT1* and *GLUT3* mRNA showed positive correlation in expression in LUAD-TCGA cohort. **1H**. GLUT1 and GLUT3 proteins showed positive correlation in expression in CPTAC-LUAD cohort.

Figure 2. **DRB18 was a more stable and more potent anticancer compound than WZB117**. **2A**. Structures of WZB117 and DRB18. **2B**. Potency of WZB117 against NSCLC A549 cells decreased after 12 hours of pre-incubation in serum-containing media. **2C**. Potency of DRB18 against NSCLC A549 cells did not change after 72 hours of pre-incubation in serum-containing media. **2D**. Comparison of potencies between DRB18 and WZB117 in NCI60 cancer cell line panel shows that DRB18 was a more potent anticancer compound compared to WZB117. **2E**. DRB18 reduced the viability in A549 NSCLC cells after 24, 48 and 72 hours of treatment in dose-dependent manner. **2F**. DRB18 reduced intracellular glucose uptake in A549, H1299, Hela, Panc1, HOP92 and INS1 cancer cells in a dose-dependent manner.

Figure 3. **DRB18 potency changed with alterations in extracellular nutrients *in vitro* in A549 and Panc1 cancer cells.**

3A. Relative intracellular ATP (iATP) changes with increasing concentrations of DRB18 (0, 10 and 20 µM) under conditions of high glucose (25 mM), low glucose (5 mM) and 0.5 mM extracellular ATP (eATP) in A549 cells. **3B.** Relative iATP changes with increasing concentrations of DRB18 (0, 10 and 20 µM) under conditions of high glucose (25 mM), low

glucose (5 mM) and 0.5 mM eATP in Panc1 cells. **3C.** Relative intracellular iATP changes with increasing concentrations of DRB18 (0, 10 and 20 μM) under conditions of high glucose (25 mM), low glucose (5 mM) and 0.5 mM eATP conditions in Hela cancer cells. **3D**. Relative cell viability in A549 NSCLC cells after 10 μM DRB18 treatment with varying concentrations of glucose (0, 2, 10, 25 and 40 mM). **3E**. DRB18 exhibited significantly more differences in viability in A549 cells at 10-, 25- and 40-mM glucose concentrations compared to 0- and 2-mM extracellular glucose. **3F**. DRB18 inhibited total absorbance (cell viability) in A549 cells in a dose-dependent manner with varying concentrations of extracellular glutamine (0, 1, 2 and 4 mM). **3G**. Relative cell viability in Panc1 pancreatic cancer cells after 10 μM DRB18 treatment with varying concentrations of glucose (0, 2, 10, 25 and 40 mM). **3H**. DRB18 exhibited significantly more differences in viability in Panc1 cells at 10-, 25- and 40-mM glucose concentrations compared to 0- and 2-mM extracellular glucose. **3I**. DRB18 inhibited total absorbance (cell viability) in Panc1 cells in a dose-dependent manner with varying concentrations of extracellular glutamine (1, 4 mM).

Figure 4. DRB18 exhibited additive anti-proliferative effects against different cancer cell lines with several clinical and pre-clinical anticancer agents *in vitro.*

10 μM of DRB18 combined with or without other drugs to treat A549 cells for 48 hours. The inhibition of cell proliferation was compared to single compound treatment to identify anti-proliferation synergism.

4A. DRB18 combined with 10 μM V9302 showed more inhibition against A549 cells. **4B**. DRB18 combined with 100 nM or 300 nM of CB839 showed more cytotoxicity against A549. **4C**. DRB18 combined with 5 μM or 10 μM of sunitinib (Sutent) showed more inhibition against A549 cells. **4D**. DRB18 combined with 10 μM V9302 showed more inhibition against Panc1 cells. **4E**. DRB18 combined with 100 nM or 300 nM of CB839 showed more inhibition against Panc1 cells. **4F**. DRB18 combined with 5 μM or 10 μM of sunitinib showed more inhibition against Panc1

cells. **4G**. 5 µM of DRB18 combined with 0.75 µM of brigatinib showed more cytotoxicity against A549 cells. **4H**. 5 µM of DRB18 combined with 15 µM of trametinib showed more inhibition against A549 cells.

Figure 5. DRB18 exhibited anti-proliferative synergism with clinical agent paclitaxel *in vitro.*

5A. DRB18 exhibits synergism with different dosages of anticancer compound paclitaxel. **5B.** HSA model obtained synergism score of 16.57 (P-value of 0.017). **5C**. Synergistic analysis showed a synergy mean value of 44.12 suggesting very strong synergy between the DRB18 and paclitaxel. **5D**. DRB18 combined with 100 nM of paclitaxel shows more inhibition against Panc1 cells. **5E**. Low glucose (2 mM) treatment combined with 1 µM paclitaxel showed a higher anti-proliferative effect against A549 cells. **5F**. Low glucose (2 mM) treatment combined with 0.3 and 1 µM paclitaxel showed a significantly higher anti-proliferative effect against Panc1 cells.

Figure 6. DRB18 exhibited synergism of anti-tumor growth with NSCLC anticancer drug paclitaxel *in vivo*.

6A. Schematic images of tumors obtained after mice were euthanized after 5 weeks of treatment. **6B**. Combined treatment of DRB18 and paclitaxel reduced tumor volume compared to either DRB18 or paclitaxel alone or vehicle treatment. **6C**. Combined treatment of DRB18 and paclitaxel reduced tumor weight compared to either DRB18 or paclitaxel alone or vehicle treatment. **6D**. Combined treatment of DRB18 and paclitaxel increased the expression of apoptotic proteins pro-caspase 9 and pro-caspase 3 in xenograft tumors in western blot analyses.

References

1. Leiter A, Veluswamy RR, Wisnivesky JP. The global burden of lung cancer: current status and future trends. *Nat Rev Clin Onco* **2023**;20(9):624-639.

2. American Cancer Society. Key statistics for lung cancer. https://www.cancer.org/cancer/types/lung-cancer/about/key-statistics.html. **2024**.

3. Planchard D, Popat ST, Kerr K, Novello S, Smit EF, Faivre-Finn C, *et al*. Metastatic non-small cell lung cancer: ESMO Clinical Practice Guidelines for diagnosis, treatment and follow-up. *Annals Onco* **2018**;29(4):iv192-iv237.

4. Moser SS, Apter L, Solomon J, Chodick G, Wollner M, Siegelmann-Danieli N. Time on Treatment and Survival Outcomes for Patients Treated With First-line Osimertinib vs. Other Tyrosine Kinase Inhibitors, for EGFR Mutation-positive Metastatic Non-small Cell Lung Cancer: Real-world Experience Data. *Antican Res* **2024**;44(1):257-265.

5. Ye J, Wu J, Liu B. Therapeutic strategies of dual-target small molecules to overcome drug resistance in cancer therapy. *Biochem Biophys Acta Rev Can* **2023**;1878(3)188866.

6. Fernandes Neto JM, Nadal E, Bosdriesz E, Ooft SN, Farre L, McLean C, *et al.* Multiple low dose therapy as an effective strategy to treat EGFR inhibitor-resistant NSCLC tumors. *Nat Comm* **2020**;11(1):3157.

7. Nair NU, Greninger P, Zhang X, Friedman AA, Amzallag A, Cortez E *et al*. A landscape of response to drug combinations in non-small cell lung cancer. *Nat Comm* **2023**:14(1):3830.

8. Cheng F, Kovács IA, Barabási AL. Network-based prediction of drug combinations. *Nat Comm* **2019**;10(1):1197.

9. Wang X, Li Y, Qian Y, Cao Y, Shriwas P, Zhang H, *et al*. Extracellular ATP, as an energy and phosphorylating molecule, induces different types of drug resistances in cancer cells through ATP internalization and intracellular ATP level increase. *Oncotarget* **2017**;8(50):87860-87877.

10. Varghese E, Samuel SM, Líšková A, Samec M, Kubatka P, Büsselberg D. Targeting glucose metabolism to overcome resistance to anticancer chemotherapy in breast cancer. *Cancers* **2020**;12(8):2252.

11. Liberti MV, Locasale JW. The Warburg effect: how does it benefit cancer cells? *Tre Bio Sci* **2016**;41(3):211-218.

12. DeBerardinis RJ, Chandel NS. We need to talk about the Warburg effect. *Nat Metabo* **2020**;2(2):127-129.

13. Chen X, Qian Y, Wu S. The Warburg effect: evolving interpretations of an established concept. *Free Radic Biol Med* **2015**;79:253-63.

14. Medina RA, Owen GI. Glucose transporters: expression, regulation, and cancer. *Bio Res* **2002**;35(1):9-26.

15. Macheda ML, Rogers S, Best JD. Molecular and cellular regulation of glucose transporter (GLUT) proteins in cancer. *Jour cell physio* **2005**:202(3):654-662.

16. Deng D, Yan N. GLUT, SGLT, and SWEET: Structural and mechanistic investigations of the glucose transporters. *Prot Sci* **2016**;*25*(3):546-558.

17. Szablewski L. Expression of glucose transporters in cancers. *Biochem Biophys Acta Rev Can* **2013**;1835(2):164-169.

18. Ancey PB, Contat C, Meylan E. Glucose transporters in cancer–from tumor cells to the tumor microenvironment. *FEBS Jour* **2018**:285(16):2926-2943.

19. Pliszka M, Szablewski L. Glucose transporters as a target for anticancer therapy. *Cancers* **2021**;13(16):4184.

20. Reckzeh ES, Waldmann H. Development of glucose transporter (GLUT) inhibitors. *Euro Jour Org Chem* **2019**;2020(16):2321-2329.

21. Duan Sl, Wu M, Zhang ZJ*,* Chang S*.* The potential role of reprogrammed glucose metabolism: an emerging actionable codependent target in thyroid cancer. *J Transl Med* **2023**:21(1):735.

22. Tilekar K, Upadhyay N, Iancu CV, Pokrovsky V, Choe JY, Ramaa CS. Power of two: combination of therapeutic approaches involving glucose transporter (GLUT) inhibitors to combat cancer. *Biochem Biophy Acta Rev Can* **2020**;1874(2):188457.

23. Temre MK, Kumar A, Singh SM. An appraisal of the current status of inhibition of glucose transporters as an emerging antineoplastic approach: promising potential of new pan-GLUT inhibitors. *Front Pharma* **2022**;13:1035510.

24. Wang N, Zhang S, Yuan Y, Hanwen X, Defossa E, Matter H, *et al.* Molecular basis for inhibiting human glucose transporters by exofacial inhibitors. *Nat Comm* **2022**;13:2632.

25. Li YL, Weng HC, Hsu JL, Lin SW, Guh JH, Hsu LC. The combination of MK-2206 and WZB117 exerts a synergistic cytotoxic effect against breast cancer cells. *Front Pharma* **2019**:10:1311.

26. Liu Y, Zhang W, Cao Y, Liu Y, Bergmeier S, Chen X. Small compound inhibitors of basal glucose transport inhibit cell proliferation and induce apoptosis in cancer cells via glucose-deprivation-like mechanisms. *Can Lett* **2010**;298(2):178-185.

27. Galluzzi L, Kepp O, Vander Heiden MG, Kroemer G. Erratum: Metabolic targets for cancer therapy. *Nat Rev Drug Discov* **2013**;12:963.

28. Ooi AT, Gomperts BN. Molecular Pathways: Targeting Cellular Energy Metabolism in Cancer via Inhibition of SLC2A1 and LDHA. *Clin Cancer Res* **2015**;21(11):2440-4.

29. Shibuya K, Okada M, Suzuki S, Seino M, Seino S, Takeda H, *et al.* Targeting the facilitative glucose transporter GLUT1 inhibits the self-renewal and tumor-initiating capacity of cancer stem cells. *Oncotarget* **2015**;*6*(2):651.

30. Chen Q, Meng YQ, Xu XF, Gu J. Blockade of GLUT1 by WZB117 resensitizes breast cancer cells to adriamycin. *Antican Drugs* **2017**;28(8):880-887.

31. Zhao F, Ming J, Zhou Y, Fan L. Inhibition of Glut1 by WZB117 sensitizes radioresistant breast cancer cells to irradiation. *Can Chemo Pharma* **2016**;77:963-972.

32. Yakisich JS, Azad N, Kaushik V, Iyer AK. The Biguanides Metformin and Buformin in Combination with 2-Deoxy-glucose or WZB-117 Inhibit the Viability of Highly Resistant Human Lung Cancer Cells. *Stem Cells Inter* **2019**;2019(1):6254269.

33. Barron CC, Bilan PJ, Tsakiridis T, Tsiani E. Facilitative glucose transporters: Implications for cancer detection, prognosis and treatment. *Metabolism* **2016**;65(2):124-139.

34. Nakanishi Y, Iwai M, Hirotani Y, Kato R, Tanino T, Nishimaki-watanabe H, *et al*. Correlations between class I glucose transporter expression patterns and clinical outcomes in non-small cell lung cancer. Thorac Cancer **2023**;14(27):2761–2769.

35. Roberts DA, Wang L, Zhang W, Liu Y, Shriwas P, Qian Y, *et al*. Isosteres of ester derived glucose uptake inhibitors. *Bio Med Che Let* **2020**;30:127406.

36. Liu Y, Cao Y, Zhang W, Bergmeier S, Qian Y, Akbar H, *et al*. A small-molecule inhibitor of glucose transporter 1 downregulates glycolysis, induces cell-cycle arrest, and inhibits cancer cell growth in vitro and in vivo. *Mol Can Ther* **2012**;11:1672-82.

37. Shi Q, Shen Q, Liu Y, Shi Y, Huang W, Wang X, *et al*. Increased glucose metabolism in TAMs fuels O-GlcNAcylation of lysosomal Cathepsin B to promote cancer metastasis and chemoresistance. *Can Cell* **2022**;40(10):1207-1222.

38. Shriwas P, Roberts D, Li Y, Wang L, Qian Y, Bergmeier S, *et al*. A small-molecule pan-class I glucose transporter inhibitor reduces cancer cell proliferation in vitro and tumor growth in vivo by targeting glucose-based metabolism. *Can Metabo* **2021**;9(1):14.

39. Chen X, Daniels NA, Cottrill D, Cao Y, Wang X, Li Y, *et al*. Natural Compound α-PGG and Its Synthetic Derivative 6Cl-TGQ Alter Insulin Secretion: Evidence for Diminishing Glucose Uptake as a Mechanism. *Diab Metab Syndr Obes* **2021**;14:759-772.

40. Honore S, Kamath K, Braguer D, Horwitz SB, Wilson L, Briand C, *et al*. Synergistic suppression of microtubule dynamics by discodermolide and paclitaxel in non-small cell lung carcinoma cells. *Can Res* **2004**;64(14): 4957-4964.

41. Chaft JE, Rimner A, Weder W, Azzoli CG, Kris MG,CasconeT. Evolution of systemic therapy for stages I–III non-metastatic non-small-cell lung cancer. *Nat Rev Cli Onco* **2021**;18(9):547-557.

42. Sandler A, Gray R, Perry MC, Brahmer J, Schiller JH, Dowlati A, *et al*. Paclitaxel–carboplatin alone or with bevacizumab for non–small-cell lung cancer. *New Eng Jour Med* **2006**;355(24):2542-2550.

43. Demeda CF, Carvalho CHPD, Aquino ARLD, Nonaka CFW, Souza LBD, Pinto LP. Expression of glucose transporters 1 and 3 in metastatic and non-metastatic lower lip squamous cell carcinoma. *Brazilian Dent Jour* **2014**;25(5):372-378.

44. Kuo CC, Ling HH, Chiang MC, Chung CH, Lee WY, Chu CY, *et al*. Metastatic colorectal cancer rewrites metabolic program through a Glut3-YAP-dependent signaling circuit. *Theranostics* **2019**;9(9):2526.

45. Medina RA, Meneses AM, Vera JC, Guzman C, Nualart F, Astuya A, *et al.* Estrogen and progesterone up-regulate glucose transporter expression in ZR-75-1 human breast cancer cells. *Endocrinology* **2003**;144(10):4527-4535.

46. Lu J, Zhao XJ, Ruan Y, Liu XJ, Di X, Xu R, *et al.* Desloratadine ameliorates paclitaxel-induced peripheral neuropathy and hypersensitivity reactions in mice. *Acta Pha Sin* **2024**;45:1-16.

47. Cirrincione AM, Pellegrini AD, Dominy JR, Benjamin ME, Utkina-Sosunova I, Lotti F, *et al*. Paclitaxel-induced peripheral neuropathy is caused by epidermal ROS and mitochondrial damage through conserved MMP-13 activation. *Sci Rep* **2020**;10(1):3970.

48. Park SB, Goldstein D, Krishnan AV, Lin CSY, Friedlander ML, Cassidy J. Chemotherapy-induced peripheral neurotoxicity: a critical analysis. *CA: Can Jour Clin* **2013**;63(6): 419-437.

49. Ruetz TJ, Pogson AN, Kashiwagi CM, Gagnon SD, Morton B, Sun ED, *et al.* CRISPR–Cas9 screens reveal regulators of ageing in neural stem cells. *Nature* **2024**;634:1150-1157.

Acknowledgments: No acknowledgments statement.

Data availability Statement: No data has been used from repositories.

Fig 1 – GLUT1 and GLUT3 expression in LUAD patients

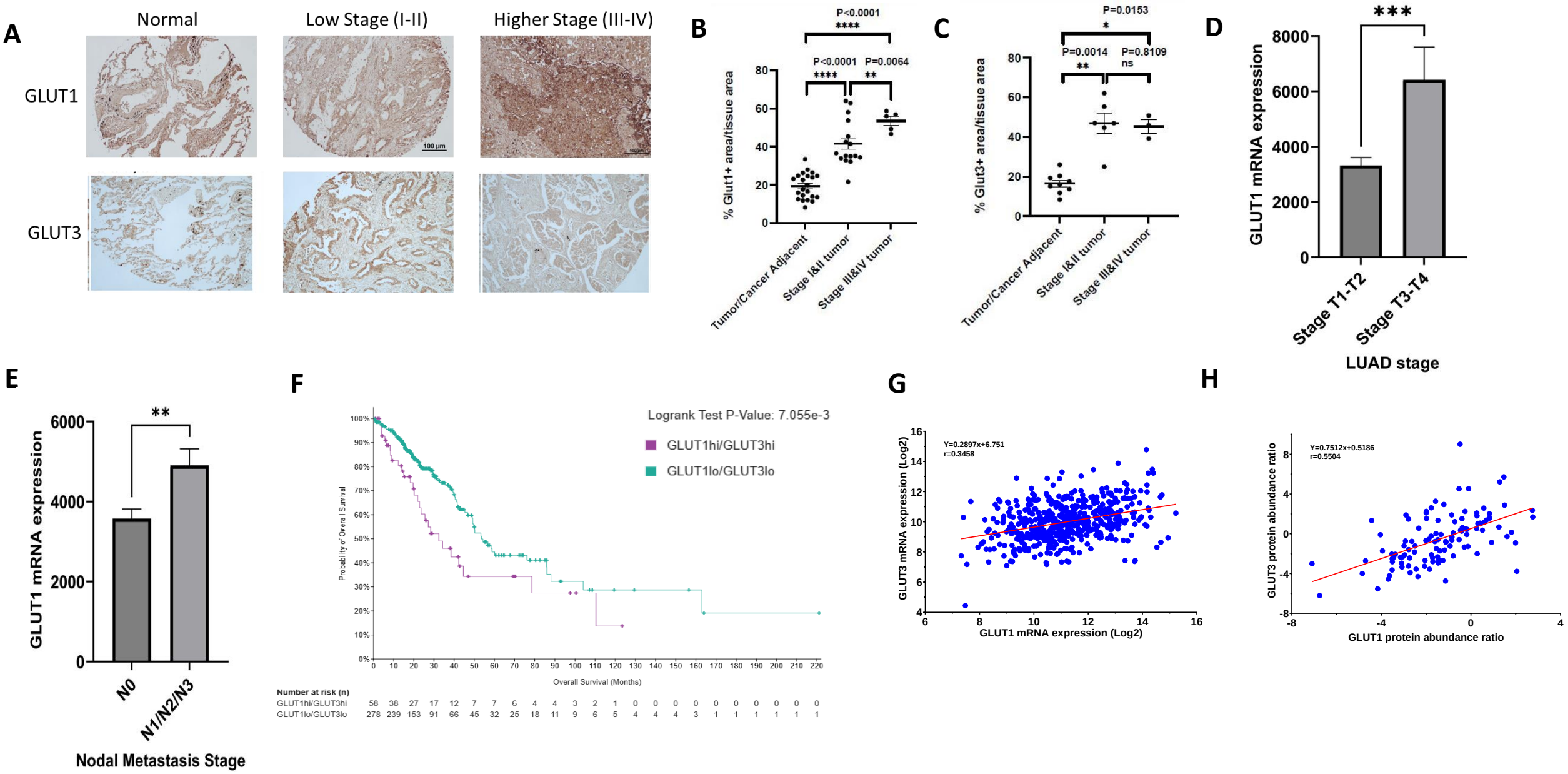

Fig 2 – DRB18 is stable anticancer compound targeting carbon-based metabolism in lung cancer

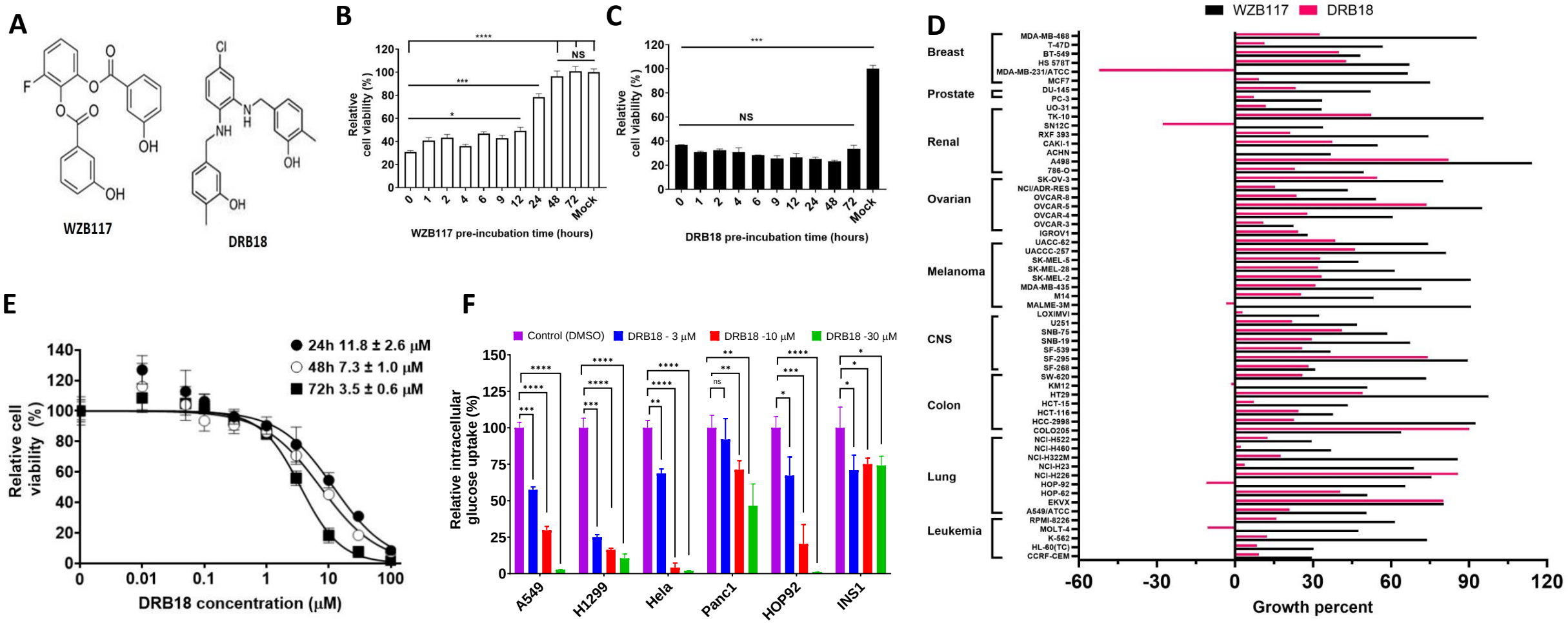

Fig 3 – DRB18 potency depends on availability of extracellular glucose and ATP

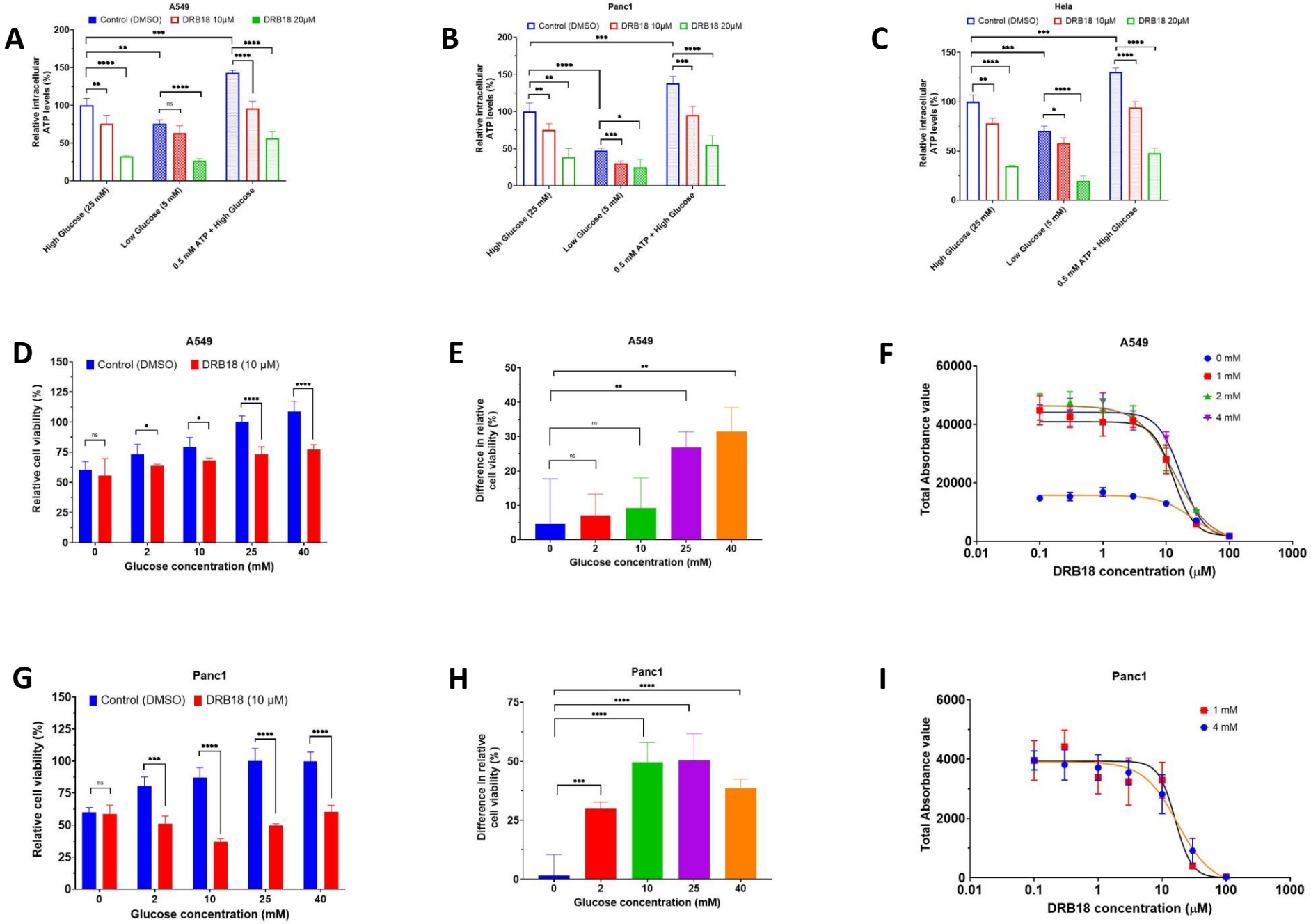

Fig 4 – DRB18 exhibits additive effect against several clinical and preclinical anticancer agents

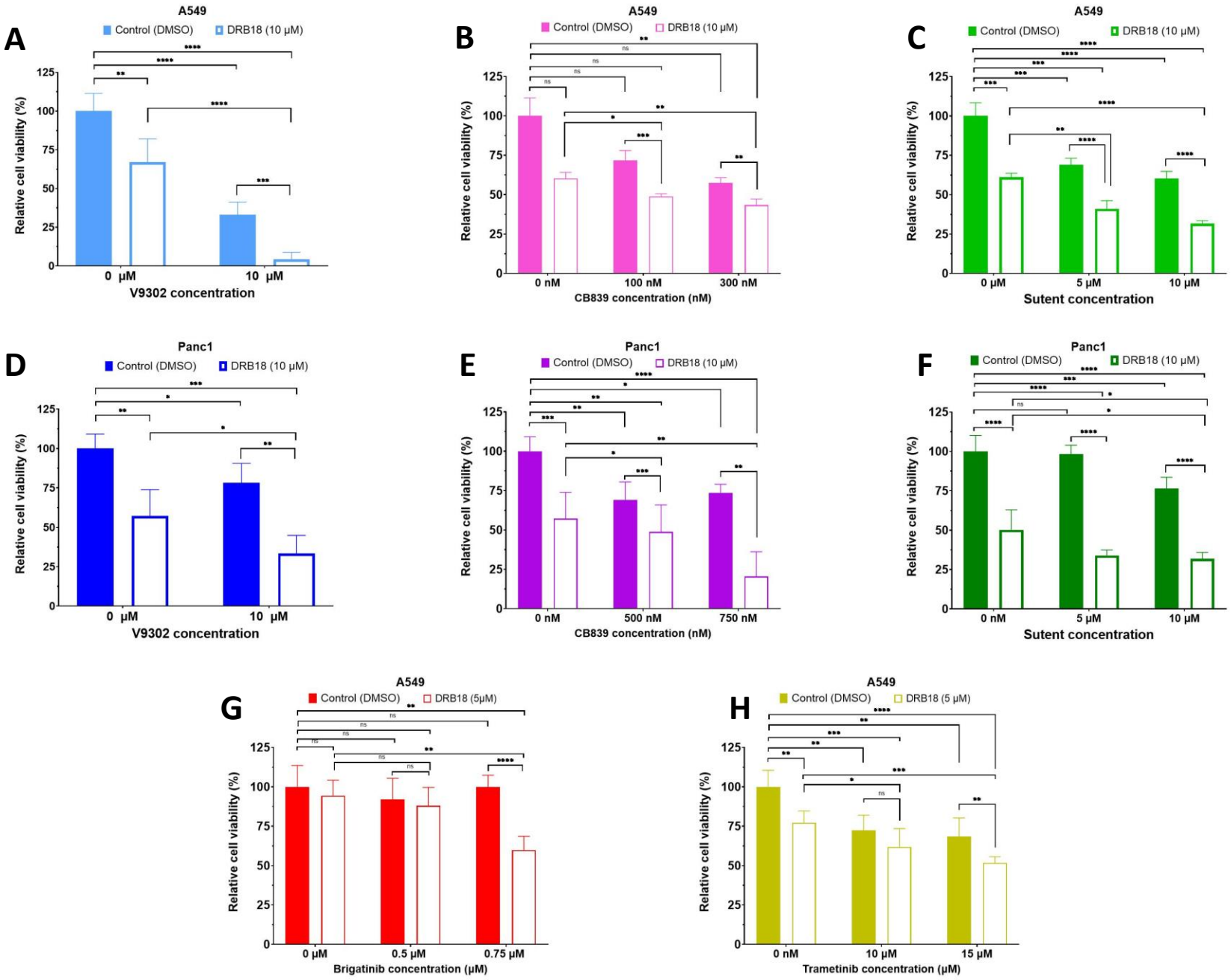

Fig 5 – DRB18 exhibits synergism with paclitaxel in vitro

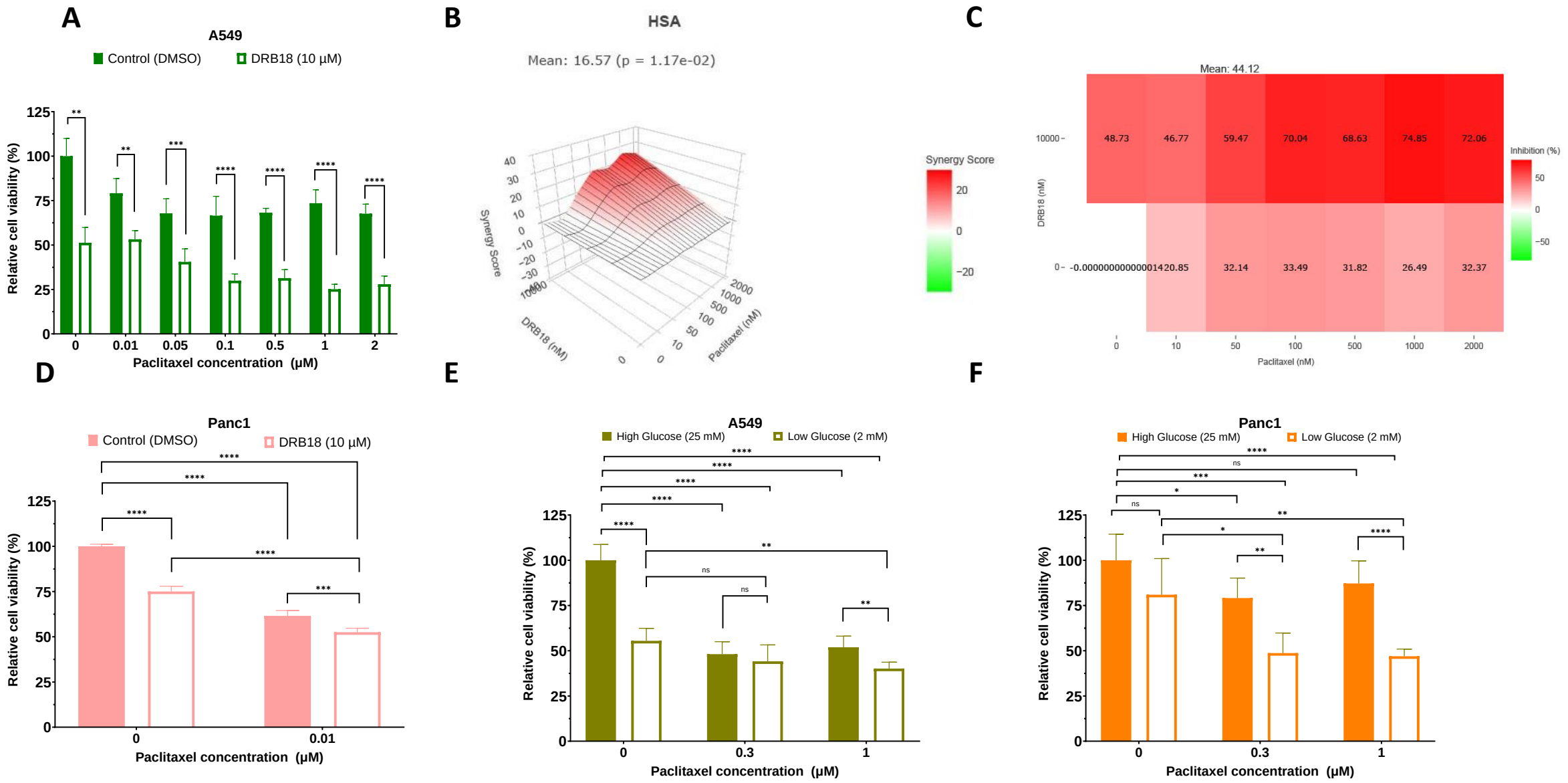

Fig 6 – DRB18 exhibits synergism with paclitaxel in vivo

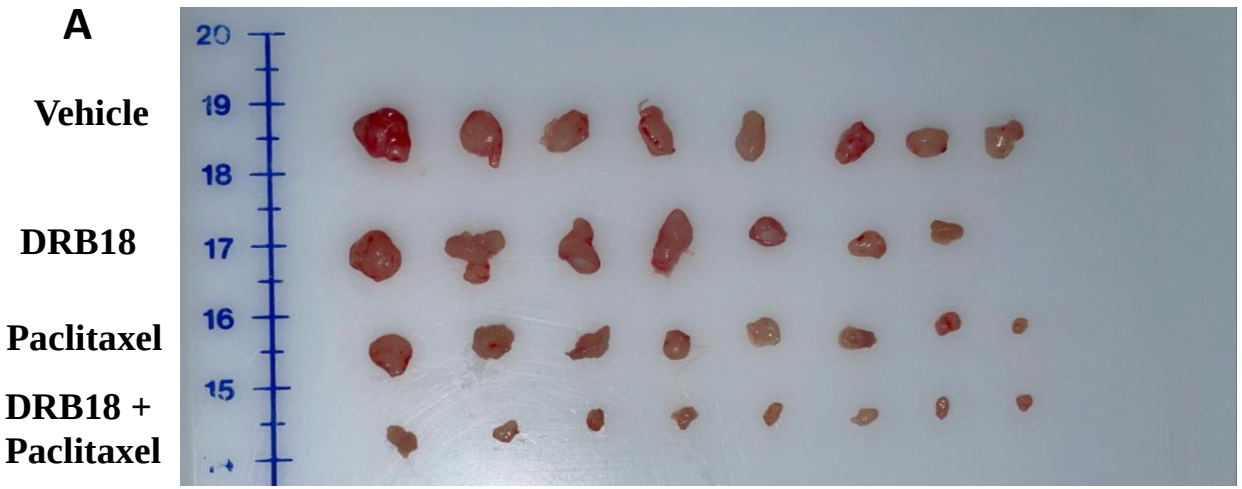

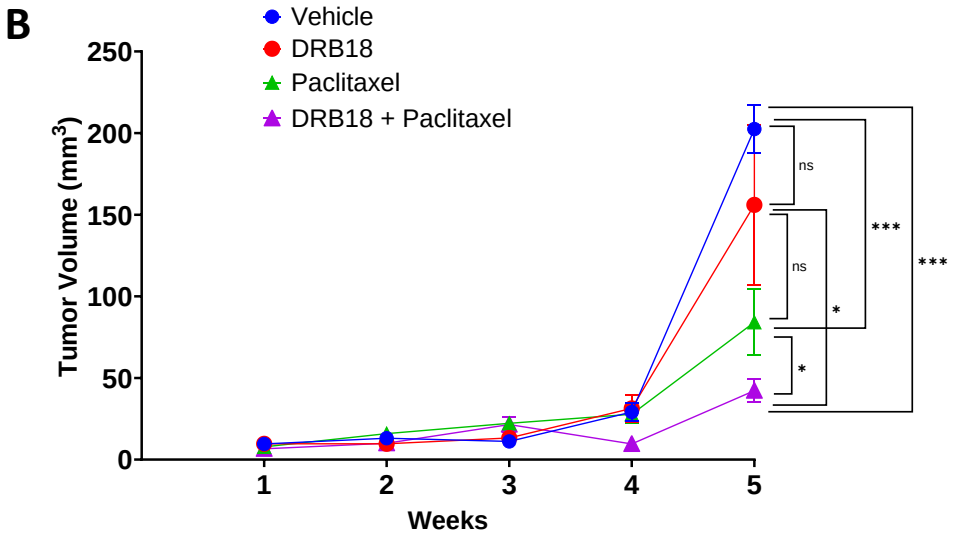

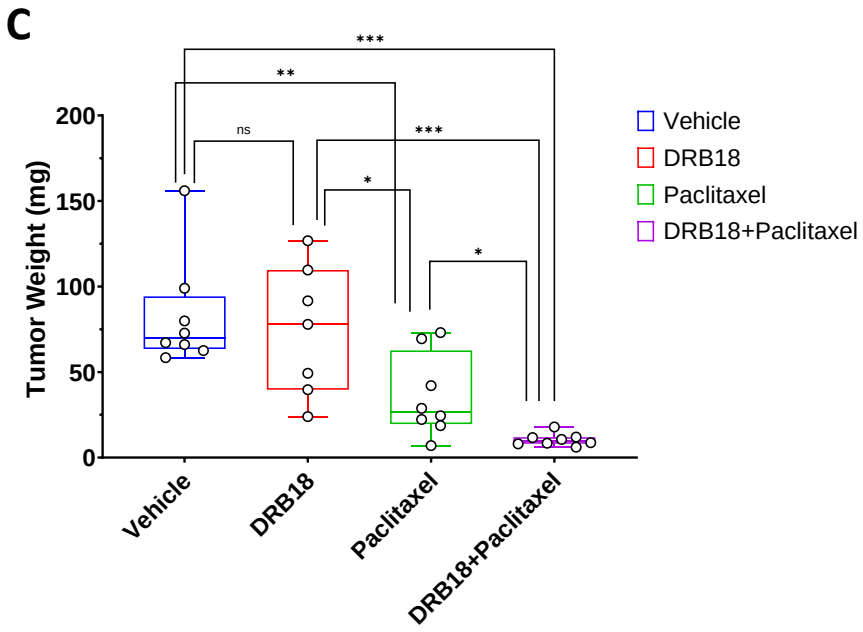

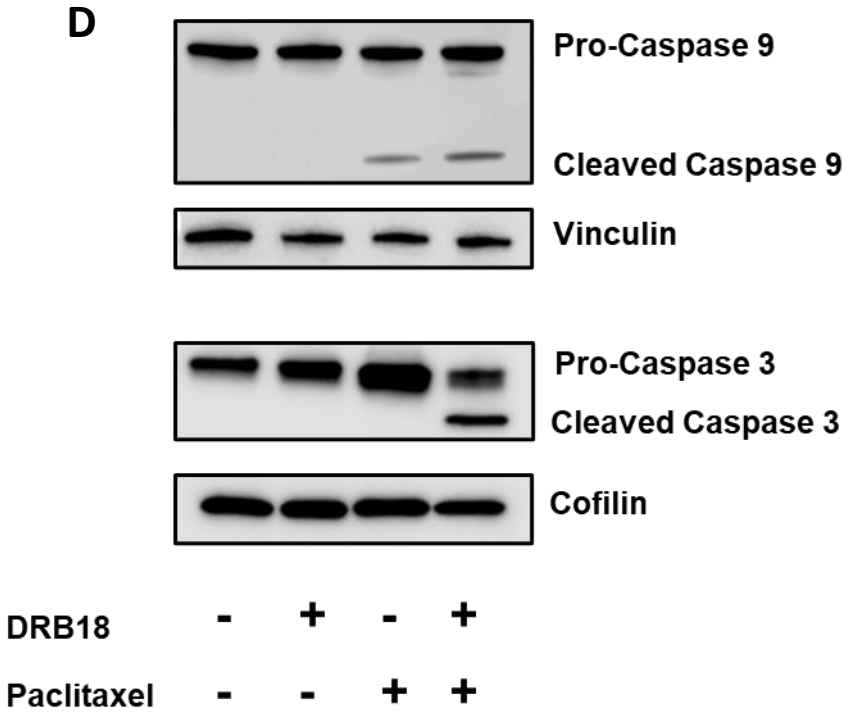

Fig S1 – Pan Cancer expression of GLUTs across TCGA cohort

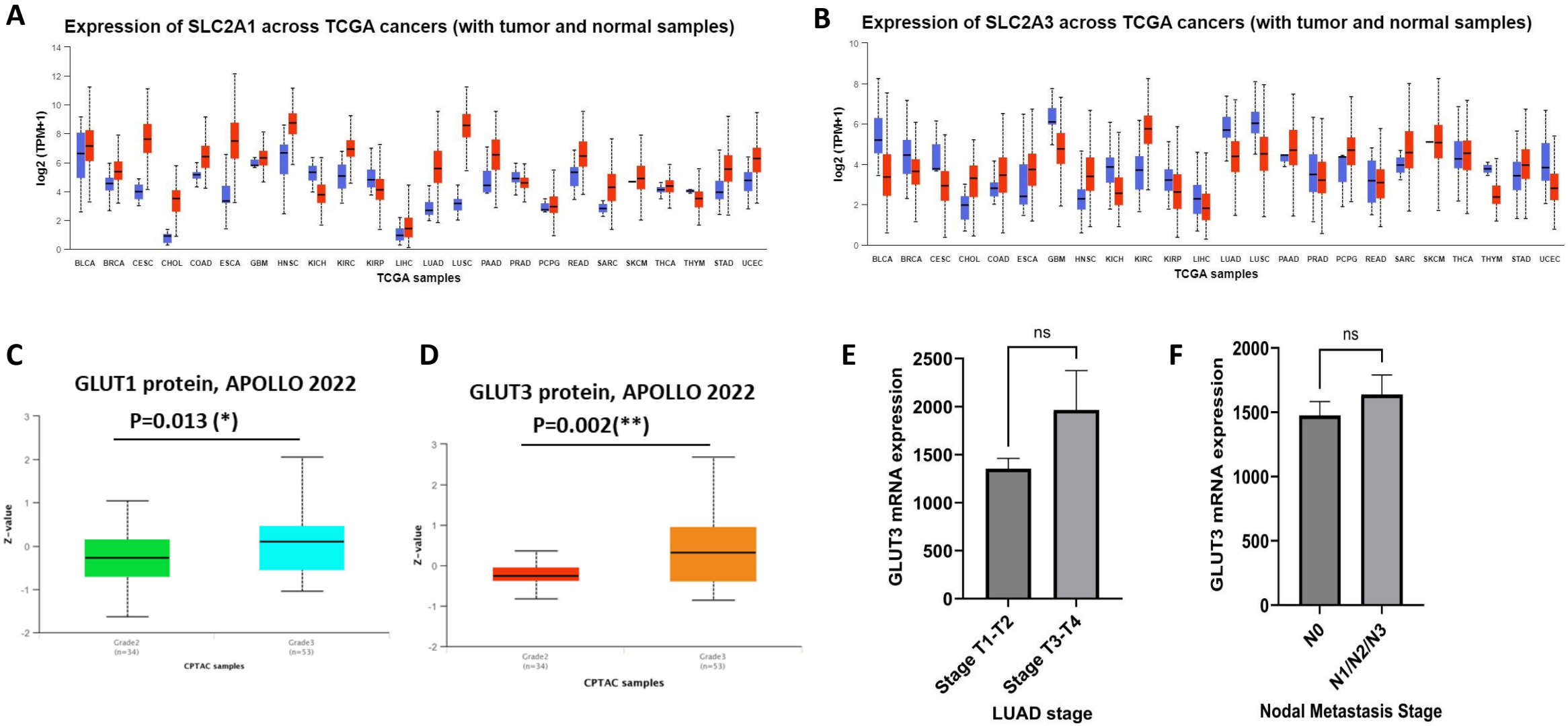

Fig S2 – GLUT1 and GLUT3 expression dependent survival and coexpression analysis

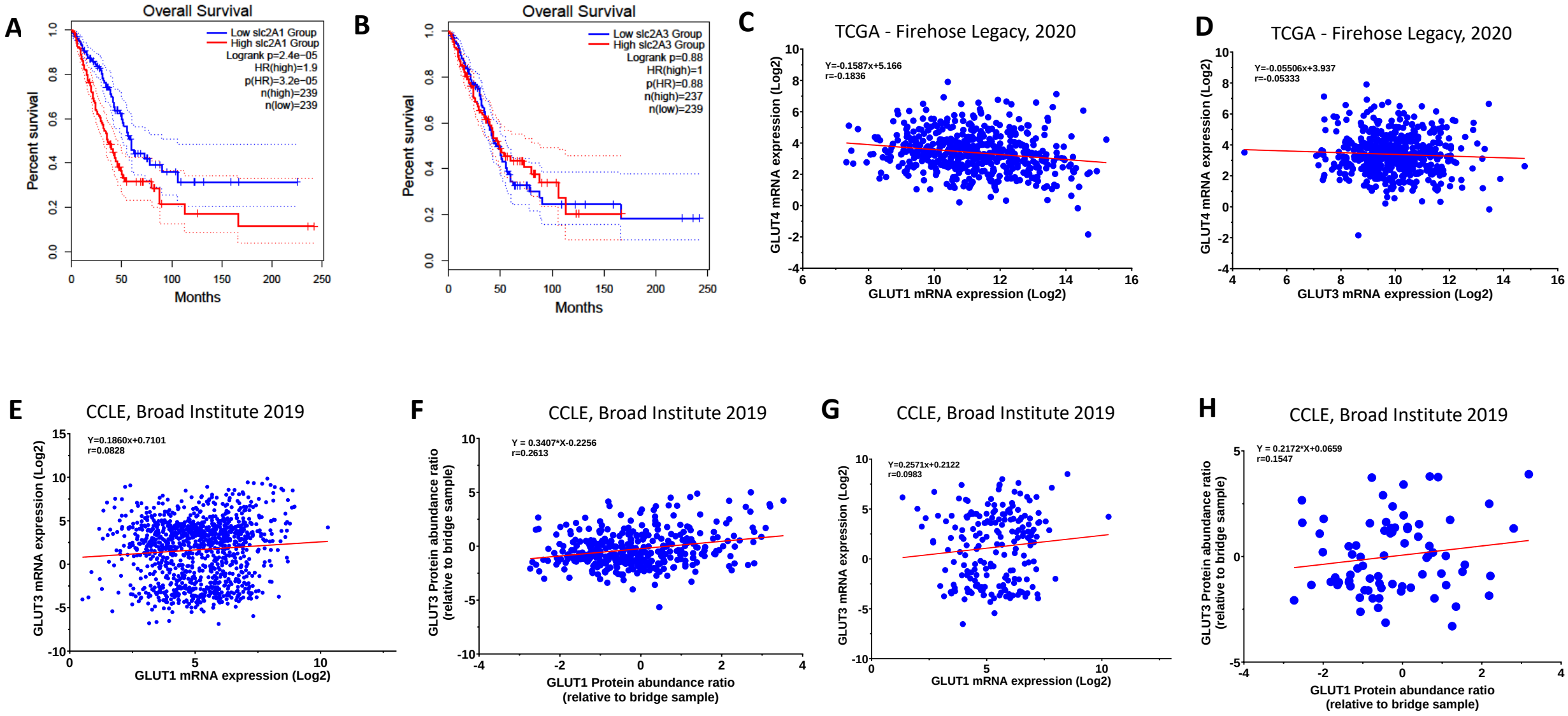

Fig S3 – GLUT1 and GLUT3 expression based on copy number alterations and mutations

A

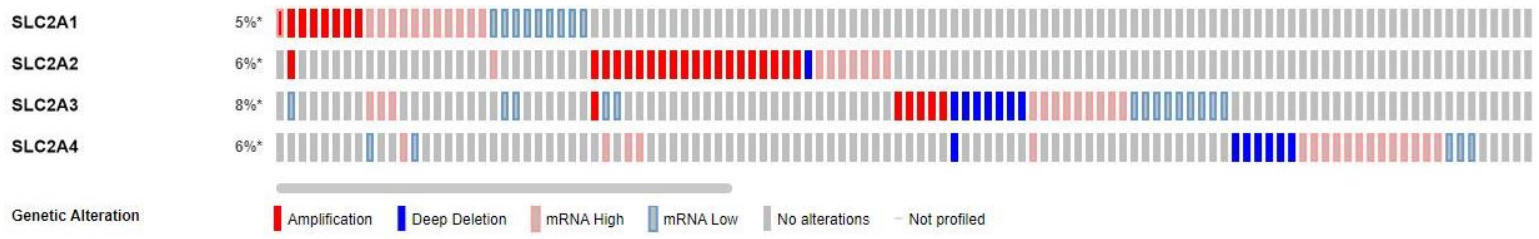

B

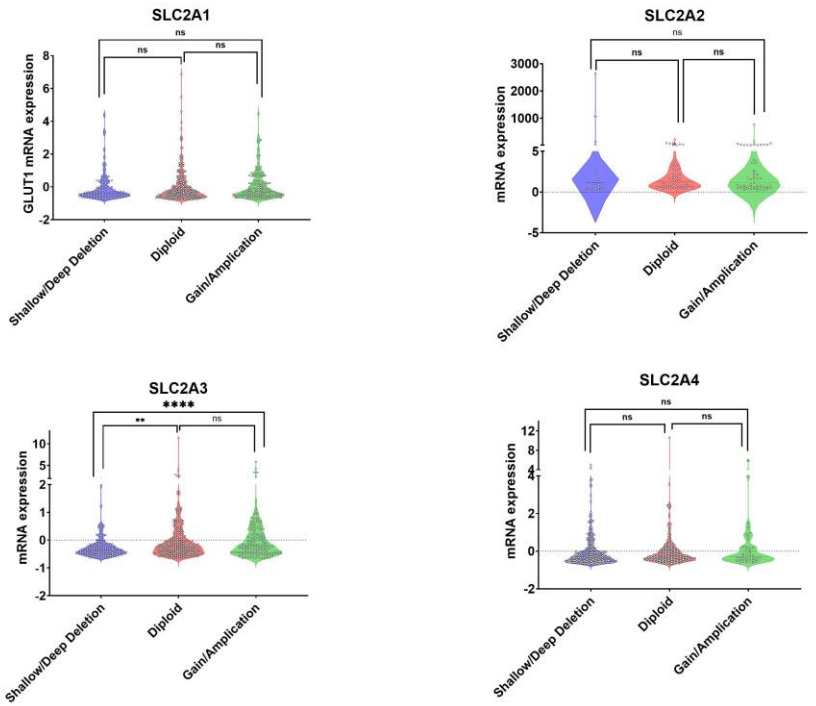

C

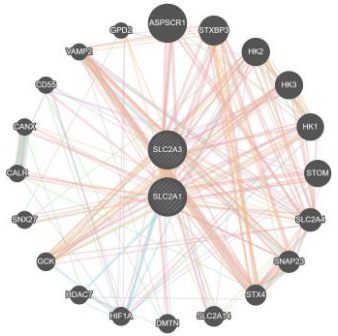

D

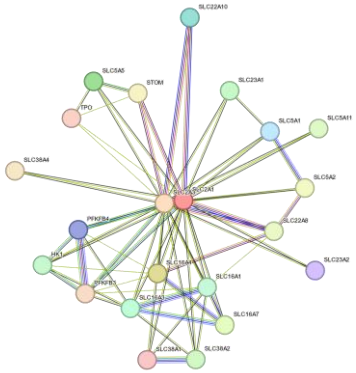

E GO database : Biological processes

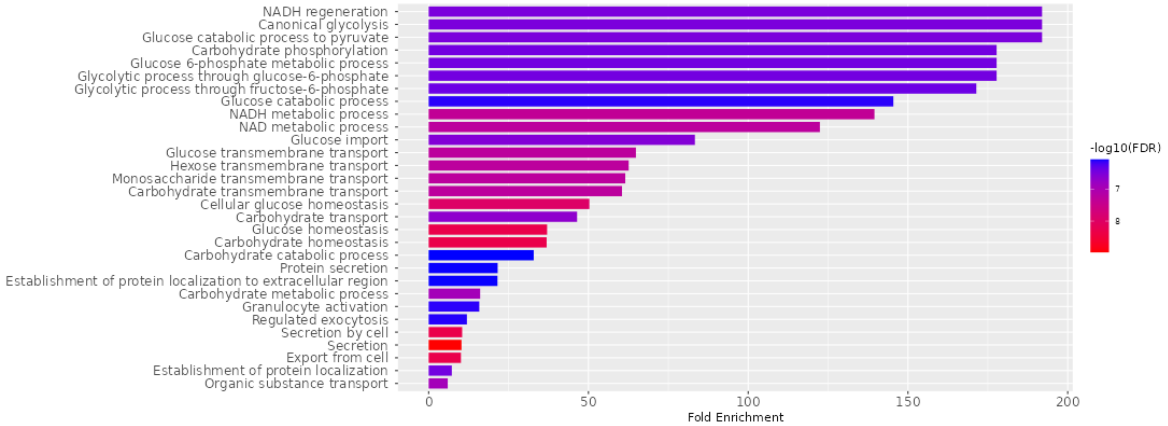

F GO database : Molecular function

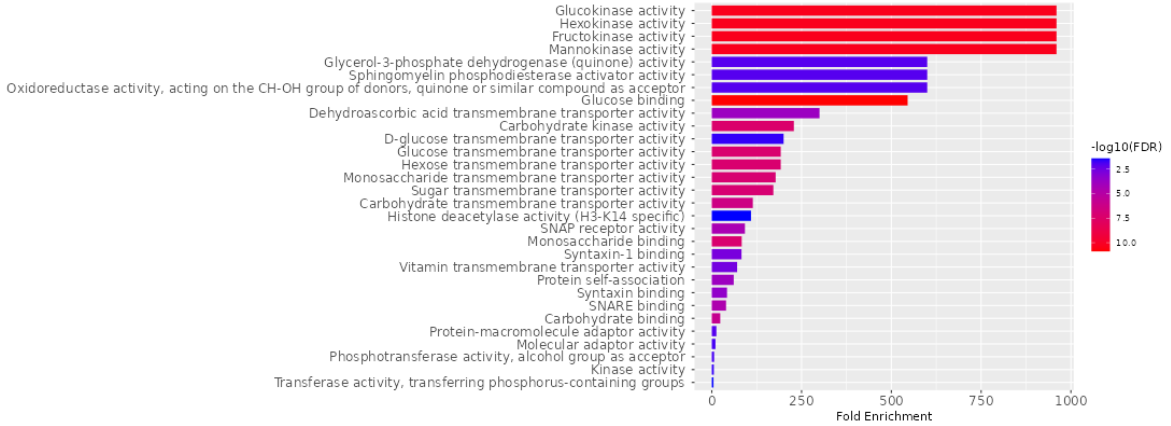

Fig S4 – Dose-dependent IC_{50} analysis of different pre-clinical or clinical anticancer agents in A549 and Panc1 cells

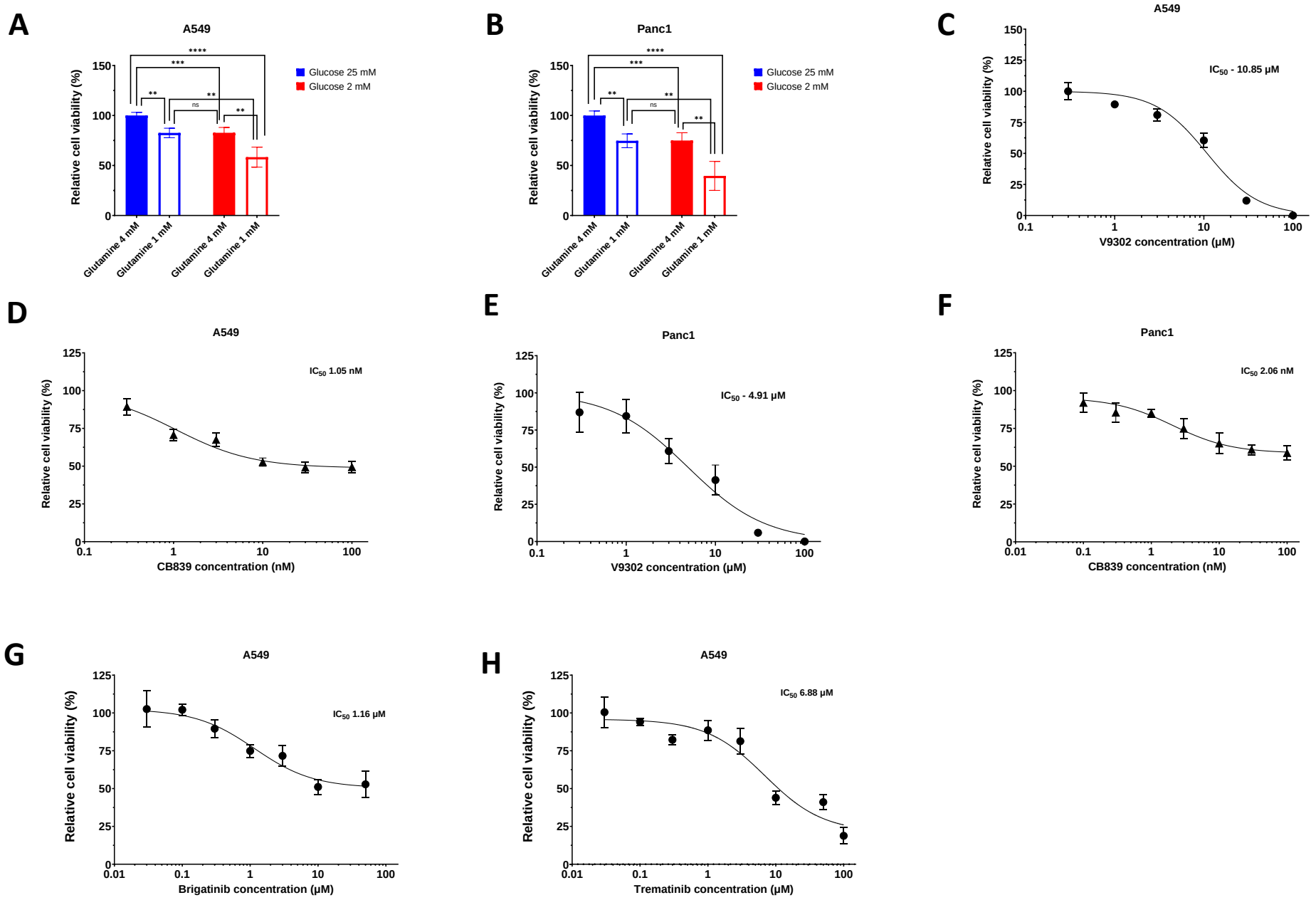

Fig S4 – Dose-dependent IC_{50} analysis of different pre-clinical or clinical anticancer agents in A549 and Panc1 cells

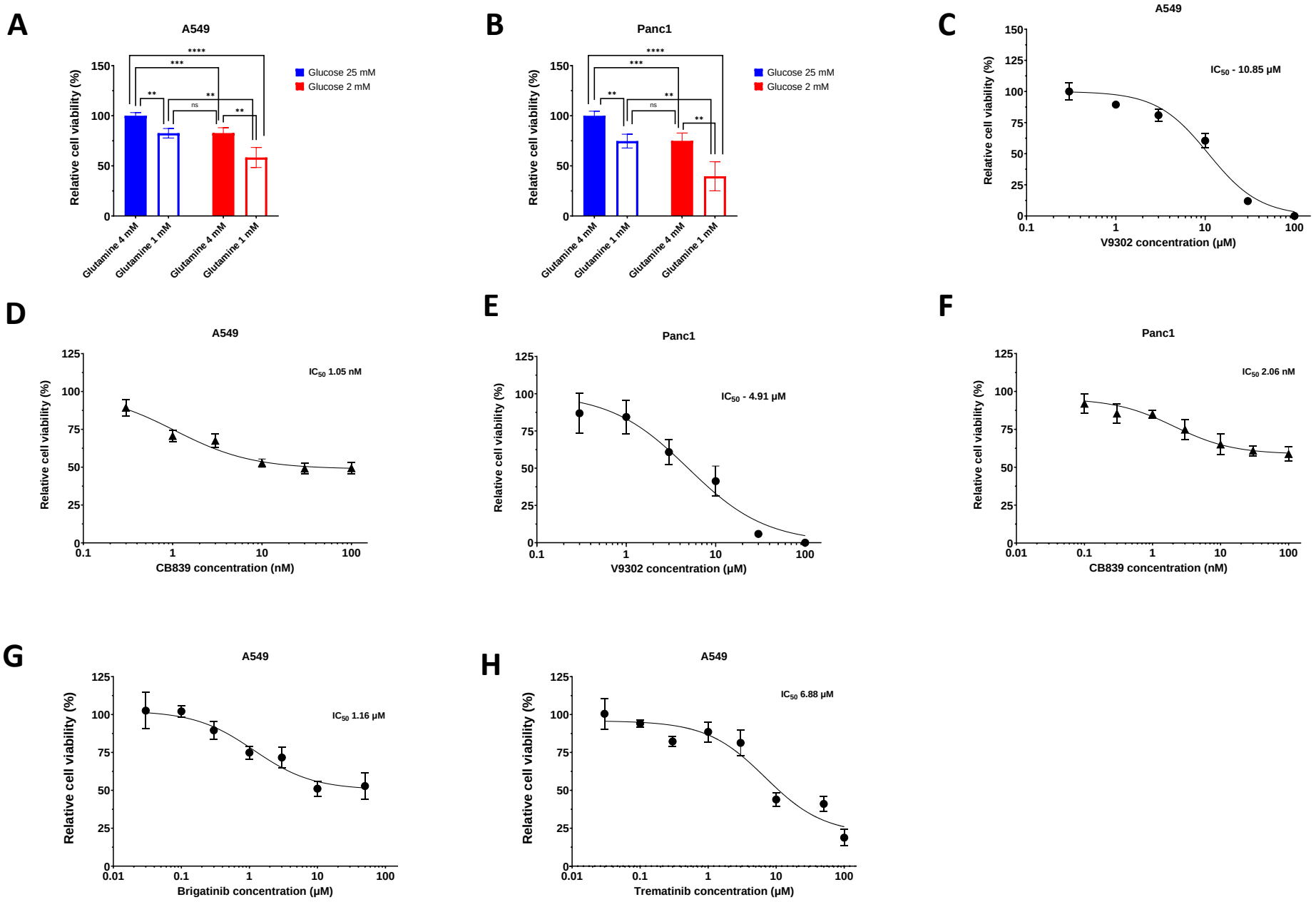
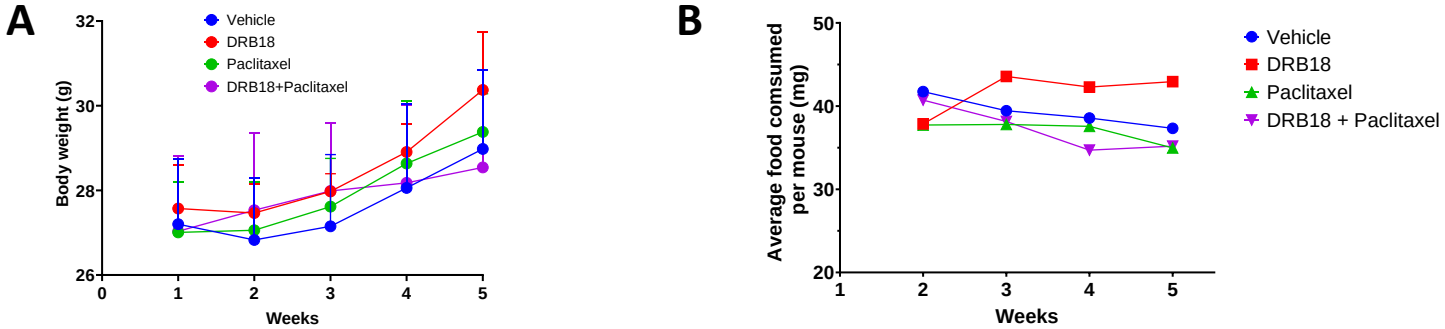
Fig S5 – Body weight and food consumption in nude mice after 5 weeks of treatment